

1 Using single remote sensing image to calculate the height of the
2 landslide dam and the maximum volume of the lake

3

4 Weijie Zou ^{1,2}, Yi Zhou ¹, Shixin Wang ¹, Futao Wang ¹, Litao Wang ¹, Qing
5 Zhao ¹, Wenliang Liu ¹, Jinfeng Zhu ¹, Yibing Xiong ^{1,2}, Zhenqing Wang ^{1,2},
6 Gang Qin ^{1,2}

7 ¹*Aerospace Information Research Institute, Chinese Academy of Sciences, Beijing, 100094, China;*

8 ²*University of Chinese Academy of Sciences, Beijing 100049, China;*

9 *Correspondence: Yi Zhou (zhouyi@radi.ac.cn) and Futao Wang (wangft@aircas.ac.cn)*

10 **1. Abstract**

11 Landslide dams are caused by landslide materials blocking rivers. After the occurrence of large-scale
12 landslides, it is necessary to conduct large-scale investigation of barrier lakes and rapid risk assessment.
13 Remote sensing is an important means to achieve this goal. However, at present remote sensing is only
14 used for monitoring and extraction of hydrological parameters at present, without prediction on potential
15 hazard of the landslide dam. The key parameters of the barrier dam, such as the dam height and the
16 maximum volume, still need to be obtained based on field investigation, which is time-consuming. Our
17 research proposes a procedure that is able to calculate the height of the landslide dam and the maximum
18 volume of the barrier lake, using single remote sensing image and pre-landslide DEM. The procedure
19 includes four modules: (a) determining the elevation of the lake level, (b) determining the elevation of
20 the bottom of the dam, (c) calculating the highest height of the dam, (d) predicting the lowest crest height
21 of the dam and the maximum volume. Finally, the sensitivity analysis of the parameters during the
22 procedure and the analysis of the influence of different resolution images is carried out. This procedure
23 is mainly demonstrated through Baige landslide dam and Hongshiyuan landslide dam. The single remote
24 sensing image and pre-landslide DEM are used to predict the height of the dam and the key parameters
25 of the dam break, which are in good agreement with the measured data. This procedure can effectively
26 support the quick decision-making regarding hazard mitigation.

27

28 **Keywords:** Landslide dam, Remote sensing, DEM, Dam height, Hazard

2. Introduction

30 Landslide dams are caused by landslide materials blocking rivers, usually in mountainous areas with
31 rivers and narrow valleys, bringing great risks to local people's lives and property(Costa and Schuster,
32 1988; Fan et al., 2020). Landslide dams disaster is widely distributed around the world. For instance, the
33 11 dams caused by the Magnitude 7.6 earthquake in New Zealand 1929(Adams, 1981); Oso Landslide
34 Dam in Washington, USA in 2014(Iverson et al., 2015); Diexi Landslide Dam on Minjiang River, China,
35 1933(Li et al., 1986); Yigong Landslide Dam in 2000(Zhou et al., 2016) and a series of landslide dams
36 including the Tangjiashan Landslide Dam caused by the Wenchuan earthquake in 2008(Zhang et al.,
37 2019).Based on the historical records of 183 landslide dams, Costa found that the main way of dam
38 breaching was overtopping. 41% of dams breached within one week, and 85% breached within a
39 year(Costa and Schuster, 1988). Respectively Fan analyzed a series of dams induced by the 2008
40 Wenchuan earthquake finding that 43% of them collapsed within one month(Fan et al., 2012). And
41 according to Shen's research on the longevity of the barrier lake, nearly 48.3% of the dams will breach
42 within a week, and 84.4% of the dams will fail within one year(Shen et al., 2020). Most of landslide
43 dams are unstable. However, the landslide dam always occurred in remote mountainous areas, with
44 inconvenient traffic conditions and poor infrastructure(Cui et al., 2009). When earthquakes or
45 precipitation induce large-scale landslides, field survey is time-consuming and manpower-
46 consuming(Dong et al., 2014). Remote areas tend to be more vulnerable and the dam breaching are more
47 likely to cause serious consequences. So, it requires us to identify the landslide dam and take action as
48 quickly as possible.

49 There are several factors influencing the process of formation, development and risk of landslide dams.
50 These factors can be divided into three categories. First, the factor of the soil, including the dam material
51 composition and the repose angle of the dam material, has an unavoidable relationship with the formation
52 and erosion process of the dan. The low permeability and high erodibility will lead to short longevity of
53 the landslide dam and fast breaching of the dam(Shen et al., 2020). Second, the hydrological parameters,
54 such as lake volume, average annual discharge and catchment area which decide the speed of lake surface
55 raising(Cao et al., 2011). The faster the lake raises, the less time is left to hazard mitigation. Third, the
56 geometric parameters, such as the length and angle of the landslide surface and the length, width, height
57 of the dam. The landslide surface influences the kinetic energy of the landslide material which has a great
58 influence on the formation of the landslide dam. And the geometric parameters of the dam itself decide
59 the stability of dam, the maximum volume of the lake and the potential maximum discharge of breaching
60 (Dong et al., 2011a; Cao et al., 2011; Shen et al., 2020).

61 Remote sensing has the ability to identify and monitor landslide dams on a large scale conveniently, and
62 supports quick decision-making regarding hazard mitigation(Canut et al., 2004; Fan et al., 2021). In the
63 research before, remote sensing is usually regarded as an auxiliary means to monitor the change of the
64 catchment area or to measure the length of the dam. For example, Wang and Lv used multiple remote
65 sensing images to extract water boundary images and pre-landslide DEM to monitor the changes of lake

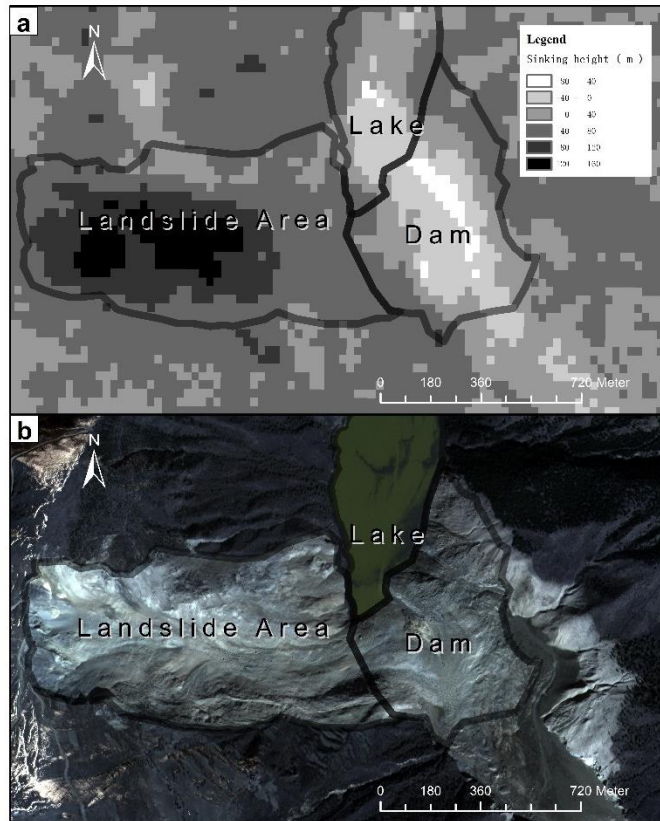
66 volume of Yigong Lake(Wang and Lu, 2002). Respectively, Cheng et al. proposed a method to estimate
67 reservoir capacity of water based on water boundary and DEM(Chen and Lu, 2008).

68 The research above focused on obtaining information about the barrier lake through remote sensing and
69 Geographic Information System. However, these kinds of methods focus on monitoring and can only
70 obtain part of geometry parameters directly through image such as catchment area. Some essential
71 components of hazard evaluation are not available in these research. Especially the height of the dam
72 which determines the maximum volume of the barrier lake and the flood peak of the dam breaching(Costa
73 and Schuster, 1988; Ermini and Casagli, 2003; Peng and Zhang, 2012; Dong et al., 2014) cannot be
74 obtained through these methods. However, as most of the landslide dams breach by overtop, they start to
75 breach as long as the elevation of lake surface equals the elevation of the landslide dam(Meng et al.,
76 2021; Costa and Schuster, 1988; Ermini and Casagli, 2003). So, the height of the landslide dam decides
77 the maximum volume of the lake. The damage of the landslide dam mostly relies on the flood it causes
78 through breaching. As water goes through the dam surface, the erosion process will lead to rapid increase
79 of the discharge and finally result in flood. According to research, his process has a strong relationship
80 with the height of the landslide dam(Anon, 2021; Shen et al., 2020; Chen et al., 2004; Braun et al., 2018),
81 which makes it one of the most important parameters related to this hazard.

82 With the rapid development of Unmanned Aerial Vehicles (UAVs), in 2008, photogrammetric UAVs are
83 also used to survey the landslide dams in the Wenchuan earthquake in 2008(Cui et al., 2009). However,
84 after the earthquake, there are to be a large number of landslides and the affected area is considerably
85 huge. If UAVs are used for precise investigation one by one, it cannot meet the requirements of timeliness
86 for the emergency. Based on the pre-landslide DTM and a series of remote sensing images after the
87 landslide dam, Dong obtains the variation of the lake level to estimate the slope foot of the barrier dam
88 and predict the dam height, completing a quick assessment of the dam breaching hazard(Dong et al.,
89 2014). But this procedure is still inconvenient as it requires sequential images to predict the height of the
90 dam. All of the methods that use the pre-landslide DEM are based on an important assumption that the
91 pre-landslide DEM is reliable. Nevertheless, take Baige Landslide Dam as an example (Fig 1), we can
92 find that the elevation of landslide area changes greatly. The landslide area has a greater degree of
93 subsidence, and the dam area has a greater degree of uplift. And even in areas nearby covered with
94 vegetation, there was about 20 meters of subsidence averagely, which demonstrates that the assumption
95 above need further improvement.

96 This research will focus on the weakness above using single remote sensing image and pre-landslide
97 DEM to obtain the essential information of the landslide dam and calculating the height of the landslide
98 dam based on the formation mechanism of the landslide dam. The Baige Landslide Dam is taken as an
99 example to verify the feasibility of this procedure. And the sensitivity analysis of the parameters during
100 the procedure and the analysis of the influence of different image resolution will be carried out in the
101 “discussion” part.

102

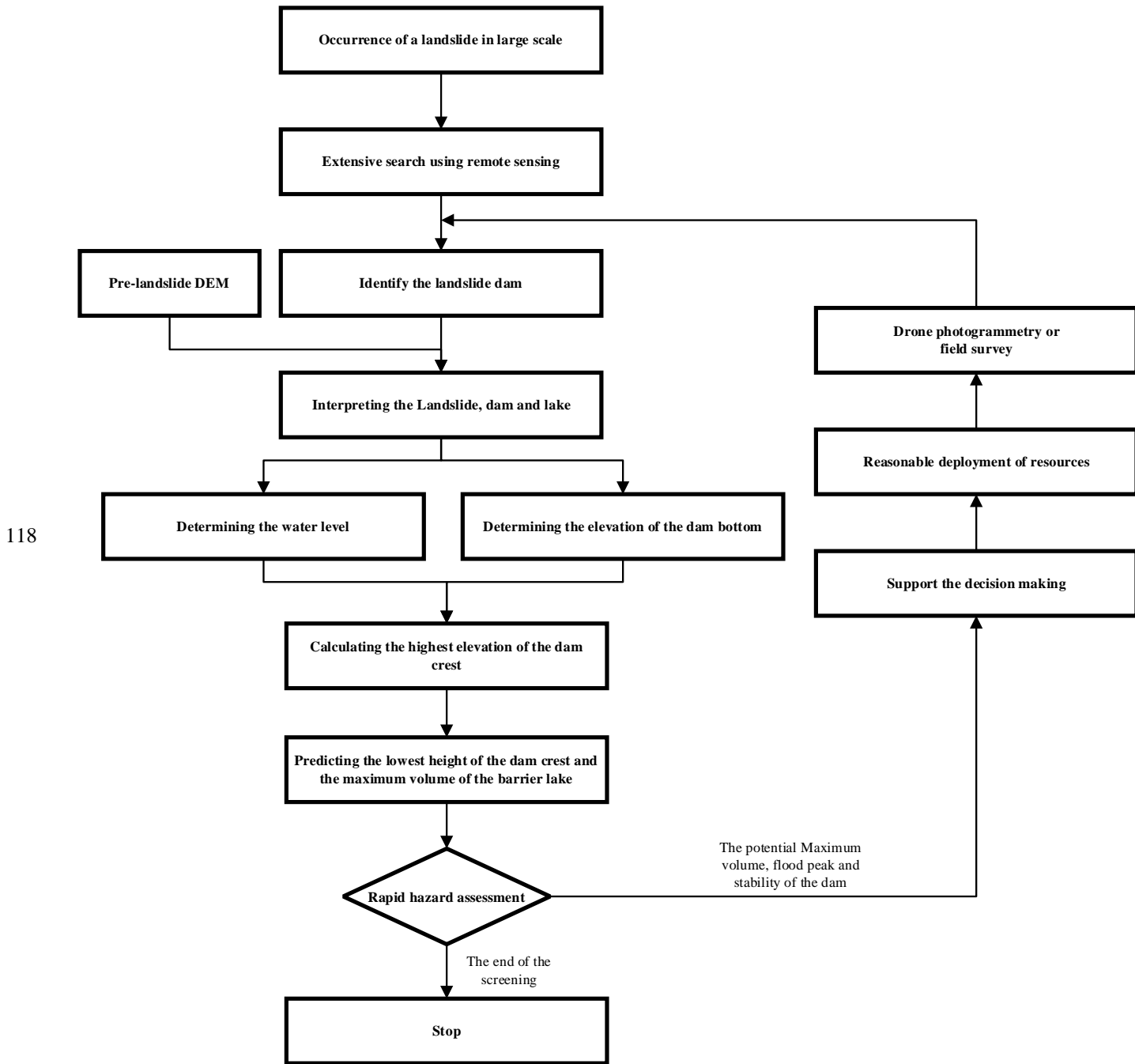


103

104 Fig 1 picture a is the comparison of pre-landslide DEM (SRTM V3) and the after-landslide DEM. And
 105 picture b is the remote sensing image from Beijing-1 satellite (taken in November 9, 2018)

106 3. Procedure

107 After the occurrence of large-scale landslides, the government often can't get all the disaster situation
 108 immediately, so large-scale landslides investigation is needed. As the disaster often occurs in remote
 109 areas, the purpose of the large-scale investigation is not only to find the landslide dams, but also to make
 110 an objective evaluation of the hazard of the landslide dams, supporting reasonable allocation of resources
 111 to avoid excessive reaction. When a landslide dam is identified from the image, the procedure to calculate
 112 its height is divided into four parts: (a) selecting the reference points to determine the elevation of the
 113 lake level; (b) estimating the elevation of the bottom of the dam; (c) calculating the highest elevation of
 114 the dam crest based on the formation mechanism of the landslide dam; (d) predicting the lowest height
 115 of the dam crest and the maximum of the lake volume. This section will elaborate the details of (a), (b),
 116 (c) and (d), obtaining the lowest height of the dam crest and calculating the maximum volume based on
 117 GIS.



119

120 Fig 2 the procedure of obtaining the height of the dam crest and completing the hazard assessment

121 3.1. Determining the elevation of the lake level

122 The method of estimating the elevation of the barrier lake based on remote sensing images has been
 123 practiced by many scholars. Typically speaking, researchers assume that the elevation of the water
 124 boundary is the same as the topography. And pre-landslide DEM is used in most cases to determine the
 125 lake level with the water boundary in the image(Wang and Lu, 2002; Chen and Lu, 2008; Dong et al.,
 126 2014; Braun et al., 2018). However, the reliability of the pre-landslide DEM may decrease as a result of

127 landslides (Fig 1). The reasons are summarized as follows: (a) the landslide has caused some changes in
128 the topography of the area; (b) the pre-landslide DEM has errors itself, especially in the mountainous
129 area; (c) as the pre-landslide DEM usually cannot be undated in time, there can be some landslides
130 without records before.

131 For the reasons above, the selection of the reference points to determine the elevation of the lake level
132 should follow these principles to reduce errors. (a) As landslides often bring about large-scale ground
133 subsidence, when selecting reference points, the point around the landslide area should be avoided. (b)
134 Because landslides and settlements tend to occur in areas with steep terrain and little vegetation
135 coverage(Ayalew and Yamagishi, 2005) and the DEM is more precise in flat terrain, the reference points
136 should be in vegetation-covered flat terrain, avoiding gully or ravines.

137 Under these strictions the reference points selected can be regarded as having the same elevation of the
138 lake level. Therefore, the lake level is determined. However, in order to determine the elevation of the
139 lake level, a complex number of reference points are needed. Their value can't be the same for the random
140 errors but should be within a certain range (Fig 7, Fig 9), for the random errors of DEM and the errors in
141 the process of determining the points. In this situation, points that are one and a half interquartile range
142 away from the mean value are considered outliers. And the elevation of the lake level is the average
143 elevation of the remains. Because the dam blocks the channel and the river has no outflow, the water
144 surface can be assumed to be still(Wang and Lu, 2002; Morgenstern et al., 2021; Fan et al., 2021). So,
145 the elevation of the lake level is the same as the elevation of the lake-dam point in Fig 3.

146 3.2. Determining the elevation of the dam bottom

147 In this procedure, the bottom of the dam refers to the point where the dam meets the river bed on the
148 downstream side. In practical cases, the most reliable method is to directly use the riverbed elevation
149 obtained recently. In the absence of relevant data, the following method should be taken for prediction.

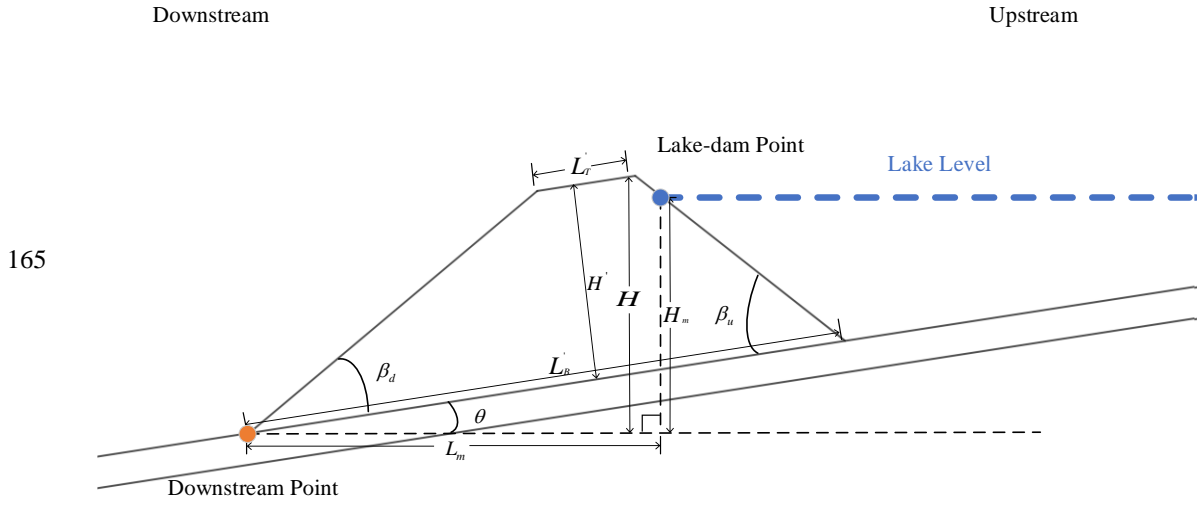
150 Within a certain range, the riverbed elevation can be considered to decrease in proportion along the
151 channel, conforming to a linear variation. Therefore, sampling elevation points at the lowest point of the
152 river valley in the pre-landslide DEM, removing the outliers and carrying out simple regression to obtain
153 the fitting of the riverbed elevation. By extending the fitting results to the dam body and subtracting the
154 historical river depth, the bottom elevation of the dam is obtained.

155 However, the historical river depth is to vary with seasons. So, there must be some errors in this prediction.
156 The influence of dam bottom elevation on calculating dam height will be analyzed in the “discussion”
157 section.

158 3.3. Calculating the highest elevation of the dam crest

159 According to Wu's laboratory experimental study, the geometrical form of the barrier dam is mainly
160 determined by landslide slope, river slope, angle of repose, earthwork amount and sliding height. (Wu
161 et al., 2020).

162 With his theory, if the river is completely blocked and the valley can be simplified into U-shape, the
 163 longitudinal section of the landslide dam can be simplified as a trapezoid(Wu et al., 2020) as shown in
 164 Fig 3. And the trapezoid will follow the following pattern.



166 Fig 3 simplified section of the landslide dam

167 The top of the dam is parallel to the bottom of the dam (Wu et al., 2020).

168 $L'_T \parallel L'_B$ (1)

169 Where L'_T is the top of the dam, L'_B is the bottom of the dam (Wu et al., 2020).

170 $\beta_d + \theta = \beta_u - \theta = \chi\varphi$ (2)

171 Where β_d is the angle between the body of the dam and the riverbed on the downstream side, β_u is
 172 the angle between the body of the dam and the riverbed on the upstream side, φ is the angle of repose
 173 of the landslide mass and χ is the parameter that fits the effect of “cut top” phenomenon. φ is
 174 determined by the nature of the soil itself and χ will be affected by landslide surface angle, landslide
 175 length and other factors(Grasselli et al., 2000). The determining of the χ can be simplified as
 176 follows(Wu et al., 2020):

177 $\chi = 0.57 + 0.51(1 + e^{\frac{(\alpha-34)}{10.50}})^{-1}$ (3)

178 where α is the angle of the landslide surface. As the angle is higher, the actual angle between the
 179 riverbed and the landslide material will be smaller and the length of the dam along the river will be longer.
 180 Normally speaking, this formula fits the actual situation well. The precise of this fitting will be discussed
 181 in the “discussion” section.

182 According to Wang's field investigation on the Wenchuan earthquake, it is found that the angle of repose
 183 of landslide dam in the Wenchuan earthquake is between 28.8° and 44.7° , with an average of 35.5° (Wang
 184 et al., 2013). In the absence of relevant data, it is recommended to use the average provided by Wang.

185 $\varphi = 35.5^\circ$ (4)

186 Wu proposed that the height of the dam has a certain relationship with the length of the bottom of the
 187 dam (Wu et al., 2020), as follows:

188 $H' = (0.37 + 1.1 \tan \theta) \cdot \tan(\beta_d + \theta) \cdot L_B' \quad (5)$

189 where H' is the height between the dam top and the dam bottom, θ is the angle of the riverbed and
 190 L_B' is the length of the dam along the river. The R^2 of formula (1) (2) (3) (5) are all greater than 0.95.
 191 As shown in Fig 3, the elevation of the dam-lake point and the elevation of the dam bottom has already
 192 been obtained before. So, H_m can be calculated and L_m can be obtained directly from the remote
 193 sensing images. According to formula (1), (2), (3), (4) and (5), using simple geometric relations, the
 194 following relation can be obtained:

195
 196 $L_B' = \frac{L_m}{\cos \theta} + \frac{\cos(\beta_u - \theta)}{\sin \beta_u} \cdot (H_m - L_m \cdot \tan \theta) \quad (6)$

197 $H_r = \sin \theta \cdot (L_B' - H' \cdot \tan \theta - H' \cdot \tan(90 - \beta_u)) \quad (7)$

198

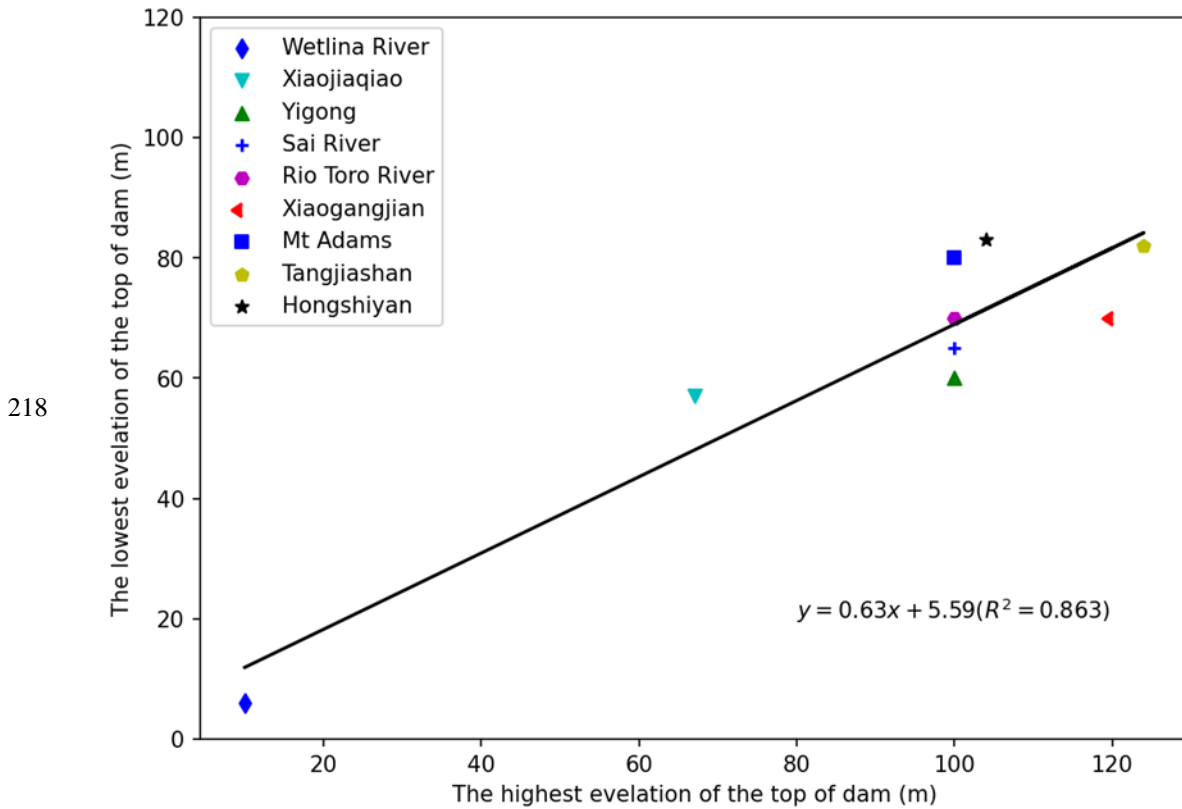
199 $H = \frac{H'}{\cos \theta} + H_r \quad (8)$

200 Where H is the difference between the highest elevation of the dam crest and the dam bottom
 201 elevation and H_r is the difference of the elevation of the riverbed between the dam bottom and the
 202 crest. θ and α can be obtained through the remote sensing image and the pre-landslide DEM easily.
 203 Through this procedure, the highest elevation of dam crest is determined based on a single image and
 204 pre-landslide DEM, which can be used in the further prediction of the dam breaching and related
 205 decision-making.

206 3.4. Predicting the lowest height of the dam crest and the 207 maximum volume of the barrier lake

208 Because the height of the landslide dam in the vertical direction of the river channel will not be
 209 consistent(Costa and Schuster, 1988; Fan et al., 2020), but will form different types of distribution
 210 according to the characteristics of the case, resulting in the height of the landslide dam is not a simple
 211 value but a range. As the most important factor affecting the dam breaching is the height of the lowest
 212 point of the dam crest, which determines the potential maximum volume of the barrier lake and the
 213 maximum discharge volume of the dam breach(Costa and Schuster, 1988; Chen et al., 2004, 2021; Dong
 214 et al., 2011b, 2014; Yang et al., 2013; Zhong et al., 2018), the prediction result of the highest elevation
 215 of the dam crest can't be used in related breaching models directly.

216 But by simply analyzing the highest elevation of the dam crest and the lowest elevation in the existing
 217 records, a simple estimation of the relationship between them is carried out, as shown in Fig 4.



219 Fig 4 the relationship between the highest elevation of the dam crest and the lowest elevation of the
 220 dam crest. These datas can be found in the papers of Cui, Costa, Mora and so on(Costa and Schuster,
 221 1991; Mora Castro, 1993; Briaud, 2008; Cui et al., 2009; Peng and Zhang, 2012; Chen et al., 2020).

222 .
 223 The relationship can be expressed as follows:

224
$$H_l = 0.63H_h + 5.59(R^2 = 0.863) \quad (9)$$

225 where H_l is the lowest elevation of the dam crest and H_h is the highest elevation of the dam crest.

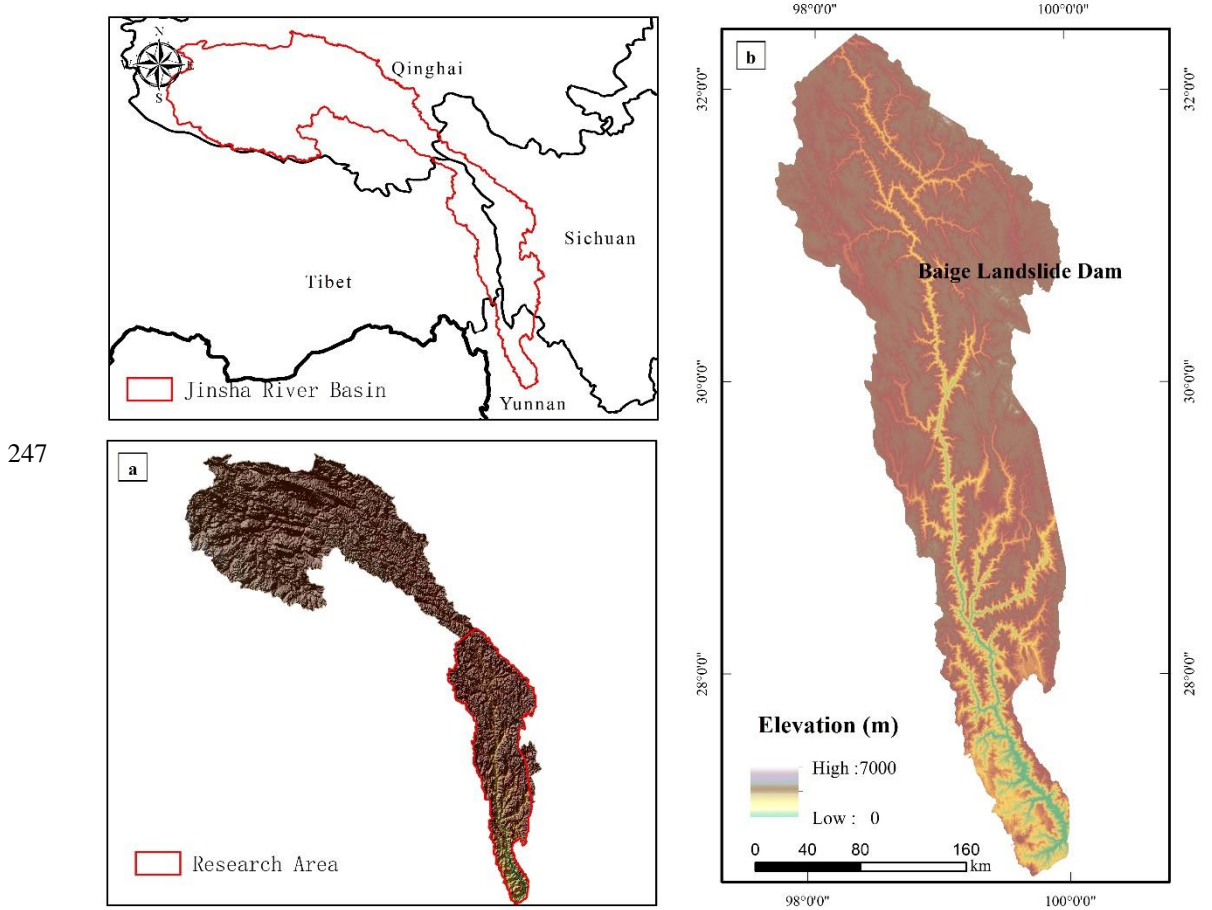
226 On the basis of the formula above, we can use the lowest elevation of the dam crest to complete the rapid
 227 assessment of the breaching hazard.

229 4. Validation of the proposed procedure

230 4.1. Baige Landslide Dam

231 The Jinsha River, the upper reach of the Yangtze River, was dammed twice recently at Baige, Tibet, one
 232 on 10 October 2018 and the other on 3 November 2018 (UTC+8), at 98°42'32.24"E, 31°4'59.27"N(Fig

233 5) (Zhang et al., 2019) and one on November 3, 2018, the residual landslide of "10.10" Baige Landslide
 234 Dam slid down again, forming "11.03" Baige Landslide Dam on the basis of the original residual dam(Li
 235 et al., 2019). The dam is much larger than the first one, as the width of the dam top is 195 m, the length
 236 of the dam top is 273 m and the highest elevation of the dam crest is 3014m(Chen et al., 2020). After
 237 proper treatment, its storage capacity is reduced from $8.69 \times 10^8 m^3$ to $5.79 \times 10^8 m^3$ and the flood
 238 peak is diminished from $41624 m^3 / s$ to $31000 m^3 / s$ (Chen et al., 2020; Yunjian et al., 2021). A
 239 large number of roads and bridges were damaged downstream, and a total of 54,000 people were affected,
 240 with economic loss of over 7.43 billion yuan(Zhang et al., 2019). Due to abundant field survey data and
 241 its great harm, Baige Landslide Dam was selected to demonstrate this procedure.
 242 Baige Landslide Dam occurred in a deep valley of the mountainous area and the barrier lake is long and
 243 narrow (Fig 6). In order to demonstrate the proposed procedure, the second Baige landslide is taken as
 244 example. The image used is a 0.8m resolution image from Beijing-1 which was taken on November 9,
 245 2018 and the pre-landslide DEM we choose is SRTM V3 of 30m resolution which was taken in 2000.
 246 The effect of the resolution of the image will be discussed in the "Discussion" section.



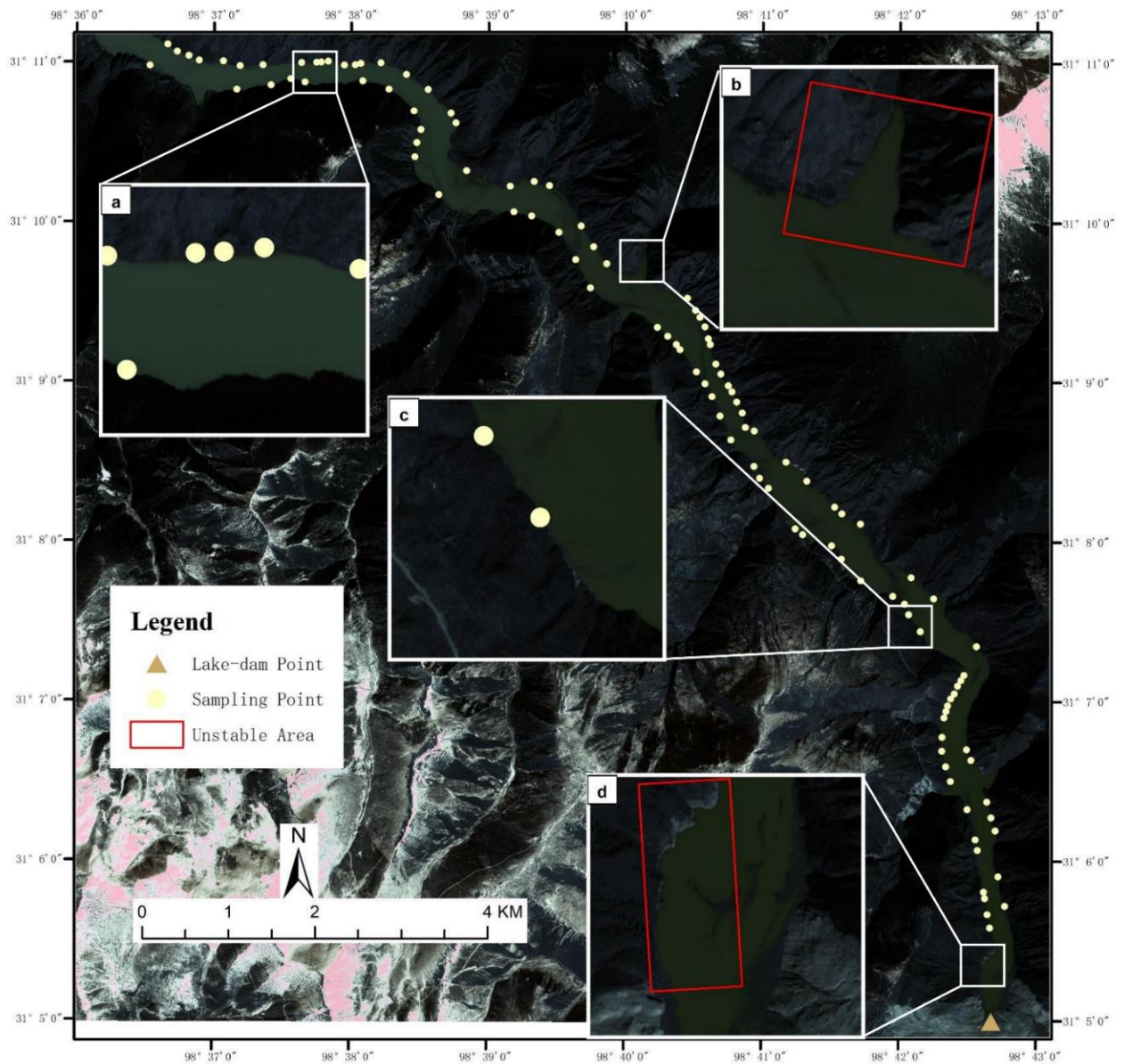
248 Fig 5 the position of the Baige Landslide Dam

249 **Determine the elevation of the lake level**

250 At the water boundary in the remote sensing image, the area covered by vegetation with relatively flat
 251 terrain and a certain distance from the landslide was selected for elevation sampling (Fig 6). Under ideal
 252 circumstances, the distribution of sampling points' elevation should be completely consistent. But in

253 practice, there are often large deviations, shown in Fig 7, the specific reasons for which have been
254 discussed in the "Procedure" section and will not be repeated. The deviation between the maximum and
255 minimum elevation of sampling points can reach 72m, and the shape basically conforms to the normal
256 distribution. Therefore, the mean of reference points can be obtained directly after clearing the outliers,
257 which is the elevation of barrier lake and the outcome is 2944m. Since the lake is essentially still, the
258 elevation of the lake should be the same as the elevation of the point where the dam meets the lake,
259 shown as the triangle in Fig 3.
260

261

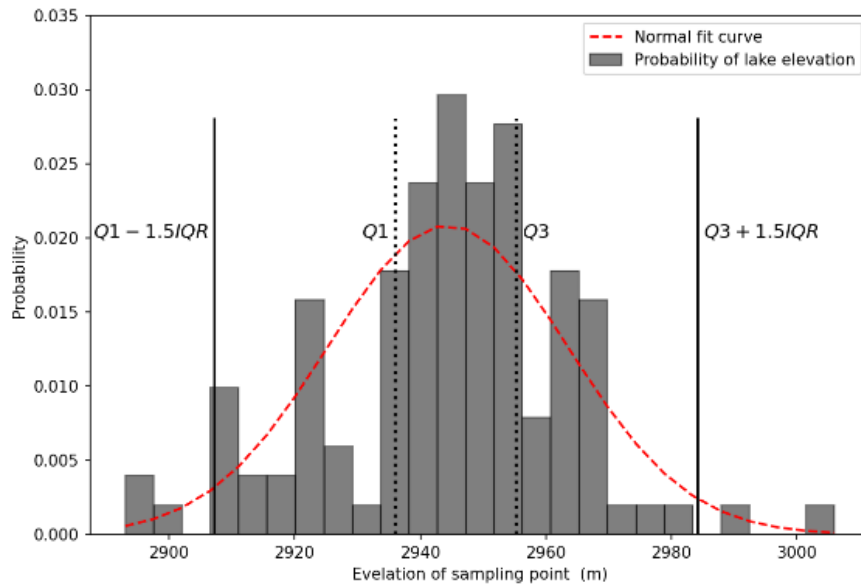


262

263

264 Fig 6 the sampling points in the case of Baige Landslide Dam (image from Beijing-1 satellite)

265



266

Fig 7 elevation distribution of sampling points in the case of Baige landslide dam

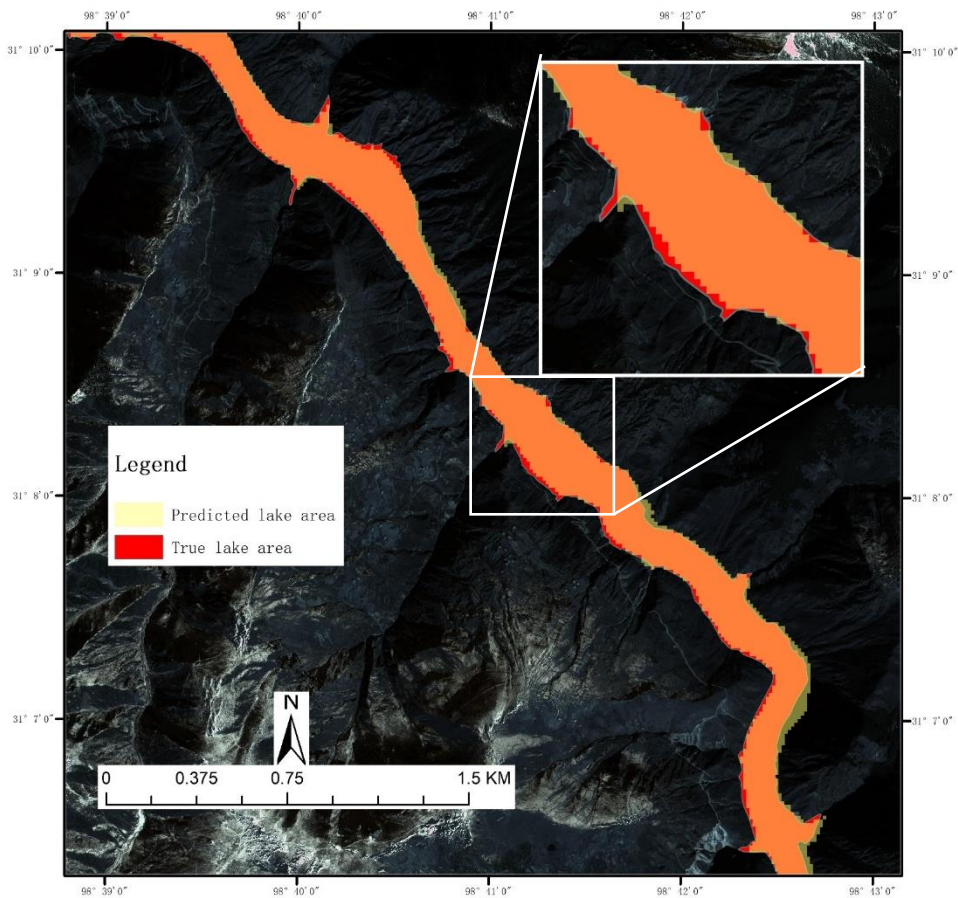
267

The Intersection over Union (IOU) of the area with elevation below 2944m in DEM and the actual submerged area in the remote sensing image is 84.48% (Fig 8). The two are found to be basically

268

269

270



271

Fig 8 the comparison of the area with elevation below 2944m in DEM and the actual submerged area

272 in the remote sensing image (image from Beijing-1 satellite)

273 **Determining the elevation of the dam bottom**

274 The inclination angle of the riverbed is calculated by sampling and unitary regression and is about 0.11° .
275 The elevation of the water level on the place of dam bottom before the landslide is 2867m. As the water
276 depth is not considered when obtaining DEM and varies with change of rainfall in the rainy season and
277 dry season, this value can't be used directly. According to the data in China Ministry of Water Resources
278 Information Center, the water depth of Jinsha River section is about 2-10m. The water depth can be
279 assumed as the mean value, 6m. Therefore, the final estimate of the dam bottom elevation is 2861m.
280 Respectively, according to the field survey, the riverbed elevation is 2860m(Chen et al., 2020).
281

282 **Calculating the highest height of the dam crest**

283 The slope angle of the landslide surface, the inclination angle of the riverbed and the length of the
284 landslide can be calculated directly through remote sensing image and DEM. The slope angle of landslide
285 surface is 30.65° . The inclination angle of the riverbed is 0.11° . And the length of the landslide that can
286 be observed is 567m. According to formula (5) (6) (7) (8), with the parameters obtained before, the
287 highest height of the dam top is 155.4m and the highest elevation of the dam top is 3016.5m with an error
288 of 2.5m compared to the measured data by Chen, 3014m(Chen et al., 2020).

289 **Predicting the lowest height of the dam crest and the maximum volume of the barrier lake**

290 Taking Baige Landslide Dam as an example, according to the case section, we have predicted that the
291 highest elevation of the dam crest is 3016.5m and the height of the dam is 155.4m. According to formula
292 (9), the lowest height of the crest of the landslide dam is 104.2m and the elevation is 2964.2m with an
293 error of 2.8m compared to the measured data by Chen, 2067m(Chen et al., 2020). Using Geographic
294 Information System, we can estimate based on DEM(Wang and Lu, 2002; Chen and Lu, 2008) that its
295 potential maximum volume is $7.96 \times 10^8 (m^3)$.

296 **4.2. Hongshiyuan landslide dam**

297 Another case for validation is Hongshiyuan landslide dam, a landslide created by moderate earthquake
298 (Ms 6.5) on August 3rd, 2014. The epicenter of the earthquake is located at 27.11° N, 103.35° E and the
299 landslide is 8.8 km southeast from the epicenter(Luo et al., 2019). The landslide dam is holding a
300 maximum water storage of $2.6 \times 10^8 (m^3)$ (Zhou et al., 2015). Breaching of this giant dam will not only
301 pose a high threat to the residents who live around, but also bring a possibility to damage other
302 hydropower dams downstream. The data used to carry out the procedure in this research and predict the

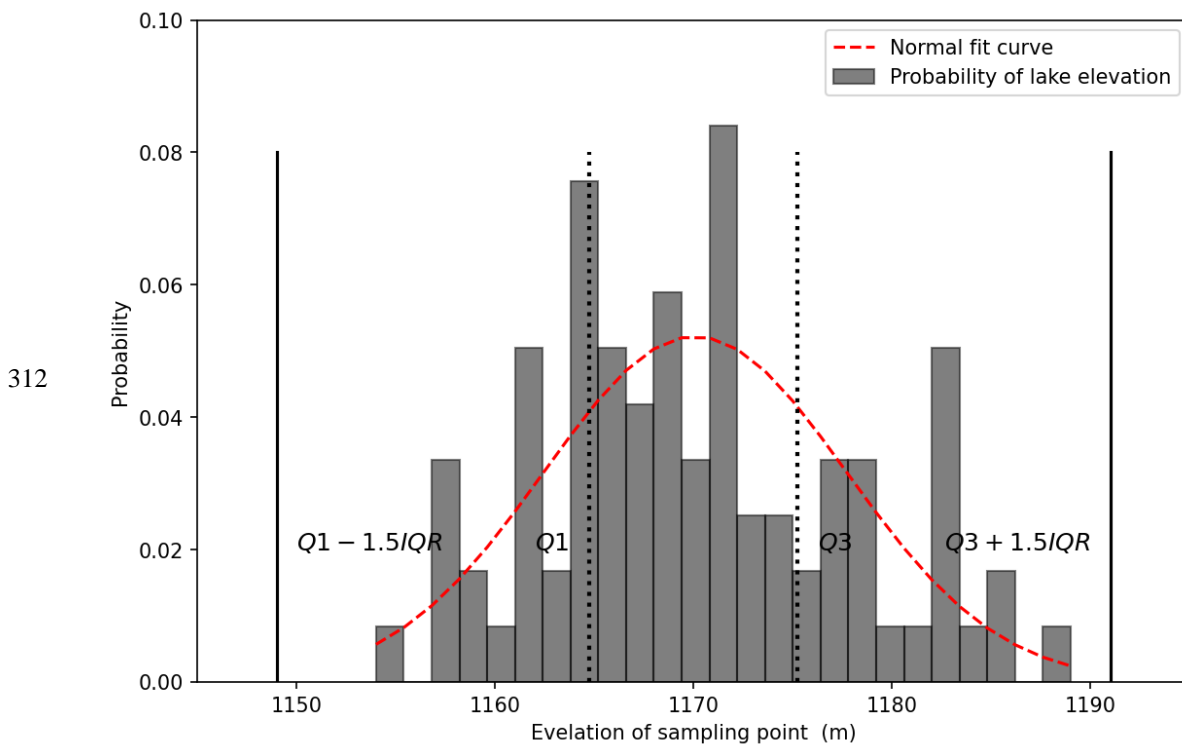
303 essential geometry parameter of landslide dam is listed in Table 1, including an after-landslide remote
 304 sensing image (2 m solution) and a pre-event DEM (30 m solution).
 305

Input data	Source	Description
After-landslide Remote sensing image	Gaofen-1 satellite	2 m solution
Pre-landslide DEM	SRTM V3	30 m solution
Repose angle of the debris	Relative case recording	Rough estimation
The elevation of riverbed	Sampling from DEM	Rough estimation

306 Table 1 Source of input data used in Hongshiyuan landslide dam case.

307 **Determine the elevation of the lake level**

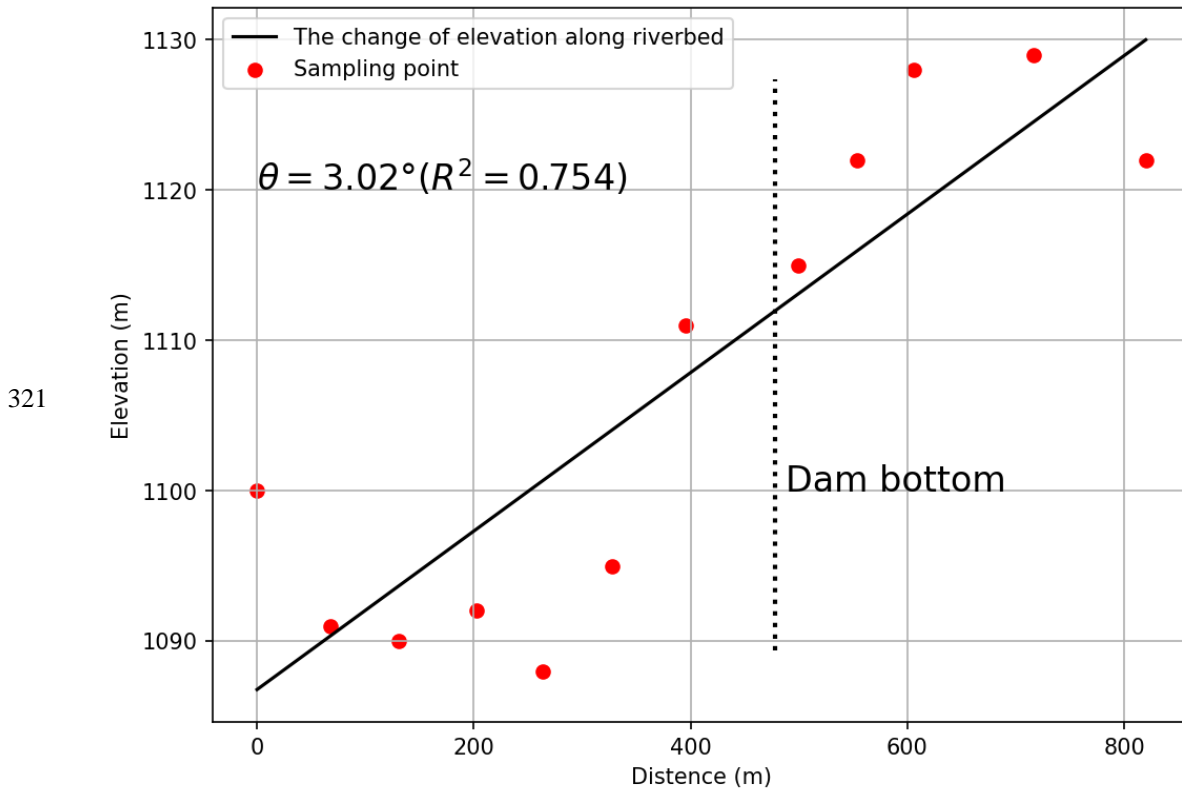
308 The image and the DEM are used to obtain the parameters required to make the prediction. The elevation
 309 of the lake level is obtained by sampling lake edge points. The distribution of the sampling points is
 310 shown in the Fig 9 and the elevation of the lake level is 1170 m.
 311



313 Fig 9 elevation distribution of sampling points in the case of Hongshiyuan landslide dam
 314
 315

316 **Determining the elevation of the dam bottom**

317 As shown in Fig 10, the pre-event elevation of the water level on the place of dam bottom can be obtained
318 through sampling the lowest points along the riverbed in the DEM, which is 1114m. As the water depth
319 of River is about 3 m(Zhou et al., 2015), the elevation of the dam bottom is 1111m.
320

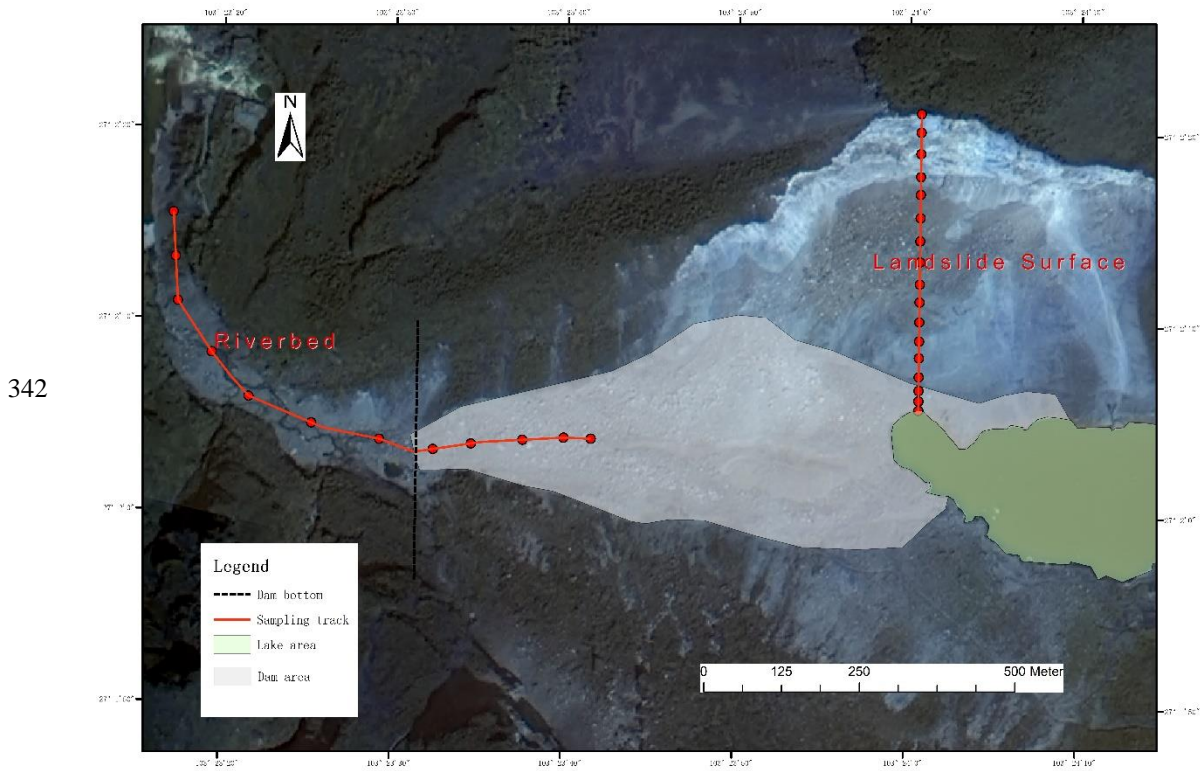


322 Fig 10 the elevation changes along the riverbed in the case of Hongshiyuan landslide dam
323

324 **Calculating the highest height of the dam crest**

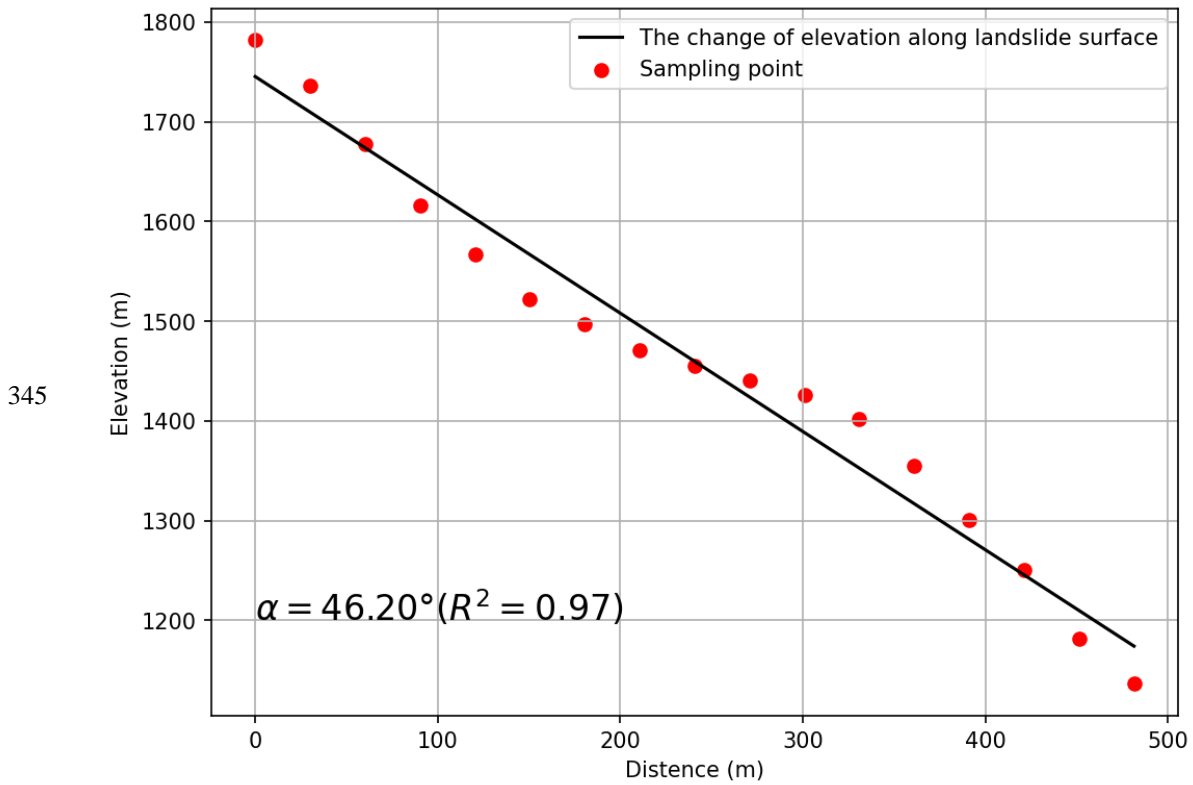
325
326 Landslide dams are caused by landslide materials blocking rivers. After the occurrence of large-scale
327 landslides, it is necessary to conduct large-scale investigation of barrier lakes and rapid risk assessment.
328 Remote sensing is an important means to achieve this goal. However, at present remote sensing is only
329 used for monitoring and extraction of hydrological parameters at present, without prediction on potential
330 hazard of the landslide dam. The key parameters of the barrier dam, such as the dam height and the
331 maximum volume, still need to be obtained based on field investigation, which is time-consuming. Our
332 research proposes a procedure that is able to calculate the height of the landslide dam and the maximum
333 volume of the barrier lake, using single remote sensing image and pre-landslide DEM. The procedure
334 includes four modules: (a) determining the elevation of the lake level, (b) determining the elevation of
335 the bottom of the dam, (c) calculating the highest height of the dam, (d) predicting the lowest crest height
336 of the dam and the maximum volume. Finally, the sensitivity analysis of the parameters during the

337 procedure and the analysis of the influence of different resolution images is carried out. This procedure
338 is mainly demonstrated through Baige landslide dam and Hongshiyuan landslide dam. The single remote
339 sensing image and pre-landslide DEM are used to predict the height of the dam and the key parameters
340 of the dam break, which are in good agreement with the measured data. This procedure can effectively
341 support the quick decision-making regarding hazard mitigation.



343 Fig 11 Hongshiyuan landslide dam (image from Gaofen -1 satellite)

344



346 Fig 12 the elevation changes cross the landslide surface in the case of Hongshiyuan landslide dam

347

348 The length of the landslide dam that can be observed, L_m , is measured directly in the image (Fig 11),
 349 which is 737.4 m. Angle of the riverbed θ which is 3.02° (Fig 10) and the landslide surface α which
 350 is 46.20° (Fig 12) can be calculated through analysis of the changes of the elevation along the river and
 351 the landslide. As the recording of the repose angle of the debris is missing, the average value of other
 352 cases is taken as a rough estimation. According to the average value of other landslide dam(Wang et al.,
 353 2013), it is set as 35.5° .

354 Putting the parameters above into the formula (6) (7) (8), we can calculate the highest elevation of the
 355 dam crest, which is 1269.9m.

356 **Predicting the lowest height of the dam crest and the maximum volume of the barrier lake**

357 As it is the lowest elevation of the dam crest that decides the break of dam, formula (9) is used to fitting
 358 the relationship between the lowest crest and the highest crest. The elevation of the lowest elevation of
 359 the dam crest is 1216.7 m. And the potential maximum volume of the lake can be calculated easily with
 360 the DEM. The comparison of field survey and predicting outcome is shown in Table 2, which suggests a
 361 strong consistency between them.

Parameter	Measured data	The predicting outcome	Error
the lowest elevation of the dam top	1222(m)	1216.7(m)	5.3(m)

the maximum of lake volume	$2.60 \times 10^8 (m^3)^*$	$3.09 \times 10^8 (m^3)$	$0.49 \times 10^8 (m^3)^*$
----------------------------	----------------------------	--------------------------	----------------------------

362 Table 2 comparison between predicting outcome and measured data from field survey(Zhou et al.,
363 2015; Luo et al., 2019)

364

365

366 5. Discussion

367 5.1. Rapid hazard assessment

368 The lowest height of the dam crest and the maximum volume of the barrier lake are important input
369 parameters for the dam-breaking model. This paper has given the procedure to obtain them rapidly. We
370 take Baige landslide dam as an example to illustrate how to use the prediction results to carry out rapidly
371 hazard assessment.

372 Many scholars have found the correlation between the geometric parameters of landslide dam and its risk
373 by empirical formula. On the basis of the prediction results and the formulas they provide, we can make
374 a quick prediction of the key information of the landslide dam hazard, such as the dam volume, the
375 stability of the barrier dam and the potential maximum discharge of the lake.

376 Predicting volume of the dam

377 The width of the barrier dam can be obtained directly from remote sensing images, which is $574.6m$.
378 As the edge and Angle conditions in the simplified model (Fig 4) have been cleared, that is, all the
379 simplified section plane parameters in the model can be obtained. So based on the relationship between
380 edges and angles in the model, the distance between top and bottom in the lowest crest, H'_l , and the
381 length of the dam top, L'_T , can be expressed by the following formula (10), (11).

$$382 H'_l = \cos \theta (0.63H_h + 5.59 - H_r) \quad (10)$$

$$383 L'_T = L'_B - \frac{H'}{\tan \beta_d} - \frac{H'}{\tan \beta_u} \quad (11)$$

384 However, because the cross section of the barrier dam is not evenly distributed in the direction of the
385 vertical river, the height change will occur as discussed in 3.5. We can assume that the change of its top
386 height is basically linear and the bottom side length and top side length of the section trapezoid do not
387 change in the direction of the vertical channel. Therefore, we can obtain the estimation Formula (12) to

388 calculate the volume of the dam debris. In the case of Baige landslide dam, the prediction outcome is
 389 $32.4 \times 10^6 m^3$, and the true value according to field survey is $30.2 \times 10^6 m^3$ (Shen et al., 2020). The
 390 error is mainly induced by the elevation change of riverbed in the direction of the vertical channel., which
 391 has a great influence to area of the dam section when the width of the dam is large.

$$392 \quad V_d = \frac{1}{4} W (H_l' + H_h') (L_B' + L_T') \quad (12)$$

393 **Predicting the stability of the landslide dam**

394
 395 In Dong research, a regression model to evaluate the stability of the barrier lake is proposed based on the
 396 case of the historical landslide dam (Dong et al., 2011a), as shown in Formula (13).

$$397 \quad L_s = -2.55 \log(P) - 3.64 \log(H_l) + 2.99 \log(W) + 2.73(L) - 3.87 \quad (13)$$

398 where P, H_l, W, L are the inflow, dam height, width and length of the landslide dam. In the case of
 399 Baige landslide. The inflow of Baige landslide dam is $822 m^3 / s$ (Li et al., 2019). The result L_s is -
 400 1.472, which means that Baige landslide dam is unstable and has a high risk to breach.

401 **Predicting the peak discharge of the breaching**

402 In the simple prediction formula (14) proposed by Cenderelli., V is the maximum volume of the dammed
 403 lake, and Q is the maximum flood peak of dam breaching. Without treatment, the largest flood peak of
 404 the Baige Landslide Dam breaching will reach $42257 (m^3 / s)$.

405

$$406 \quad Q = 3.4 \cdot V^{0.46} \quad (14)$$

407 The comparison between the predicted result and the measured date, as shown in table 3, achieves a good
 408 agreement. The rapid assessment of the dam breaching hazard has been completed. As the simulation
 409 model of dam breaching has a significant influence on the prediction of these factors, they should also
 410 be selected carefully in practical applications. Besides formulas above, there are also many other
 411 formulas to choose to complete the prediction (Costa and Schuster, 1991; Walder and OConnor, 1997;
 412 Shi et al., 2014; Ruan et al., 2021; Peng and Zhang, 2012; Zhong et al., 2018; Ermini and Casagli, 2003;
 413 Dong et al., 2011a; Shen et al., 2020). And many scholars have discussed the merits and demerits between
 414 these hazard assessment models (Peng and Zhang, 2012; Fan et al., 2021).

415

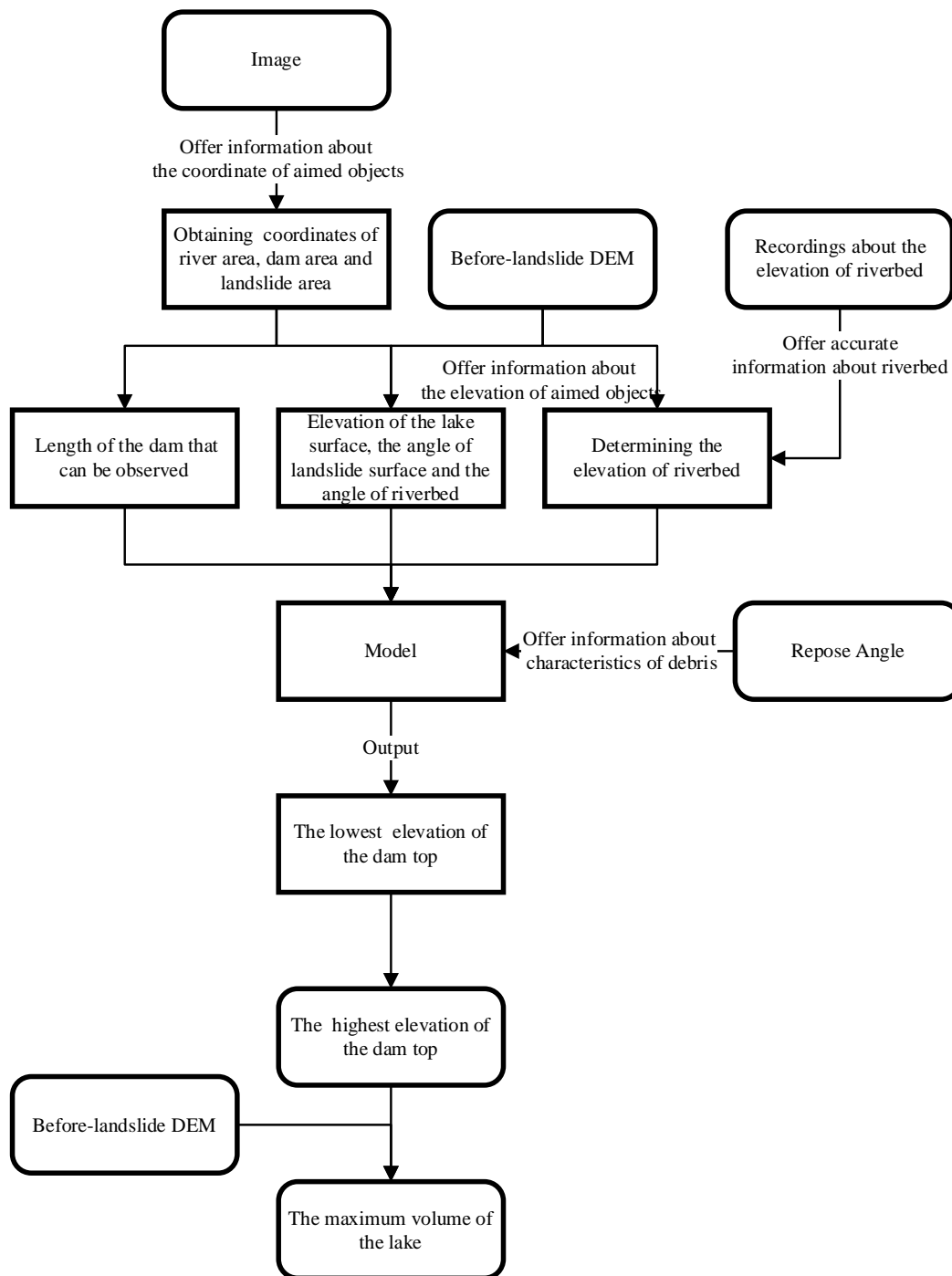
Parameter	Measured data	The predicting outcome
The highest elevation of the dam top	3014(m)	3016.5(m)

The lowest elevation of the dam top	2967 (m)	2964.2(m)
The maximum of lake volume	$8.69 \times 10^8 (m^3)^*$	$7.96 \times 10^8 (m^3)$
The dam volume	$30.2 \times 10^6 (m^3)$	$32.4 \times 10^6 (m^3)$
The stability of dam	Not stable	Not stable
The peak discharge	$41624 (m^3 / s)^*$	$42257 (m^3 / s)$

416 Table 3 the comparison of the measured data and the predicted result. As relative measures have been
417 taken to reduce the maximum volume of the barrier lake, data with star in the table is the estimation
418 results of Chen's detailed back analyses(Chen et al., 2020).

419 5.2. Sensitivity analysis

420 This study provides a method to predict critical information about a barrier dam using limited real-time
421 data. The data required includes an after-landslide satellite image and a pre-event DEM. The data that
422 is not required include the repose angle of the nearby material and the elevation of the riverbed. If there
423 are reliable recordings, they can be used in the procedure to improve the prediction accuracy.
424 Otherwise, our research provides a reliable method to predict them. The process of using of each input
425 data, determination of intermediate parameters and final output results is shown in Fig 13.



426

427

Fig 13 the complete process of parameters determination

428

429

In this procedure, the main parameters put into the model include: the length of the dam that can be

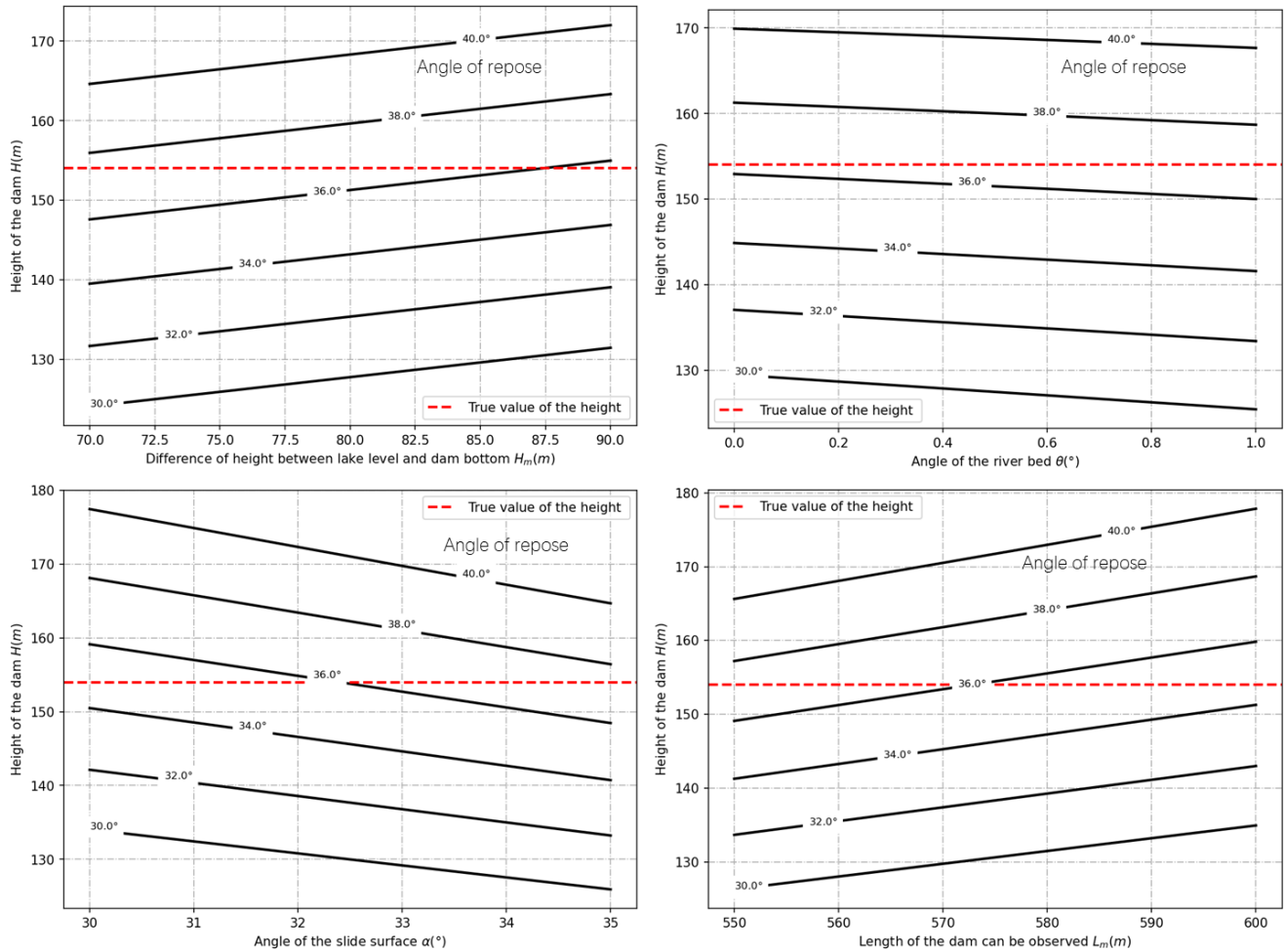
430

observed, the elevation of the lake level, the elevation of the dam bottom, the slope angle of landslide

431

surface and the inclination angle of the riverbed. Since H_m is the lake level elevation minus the

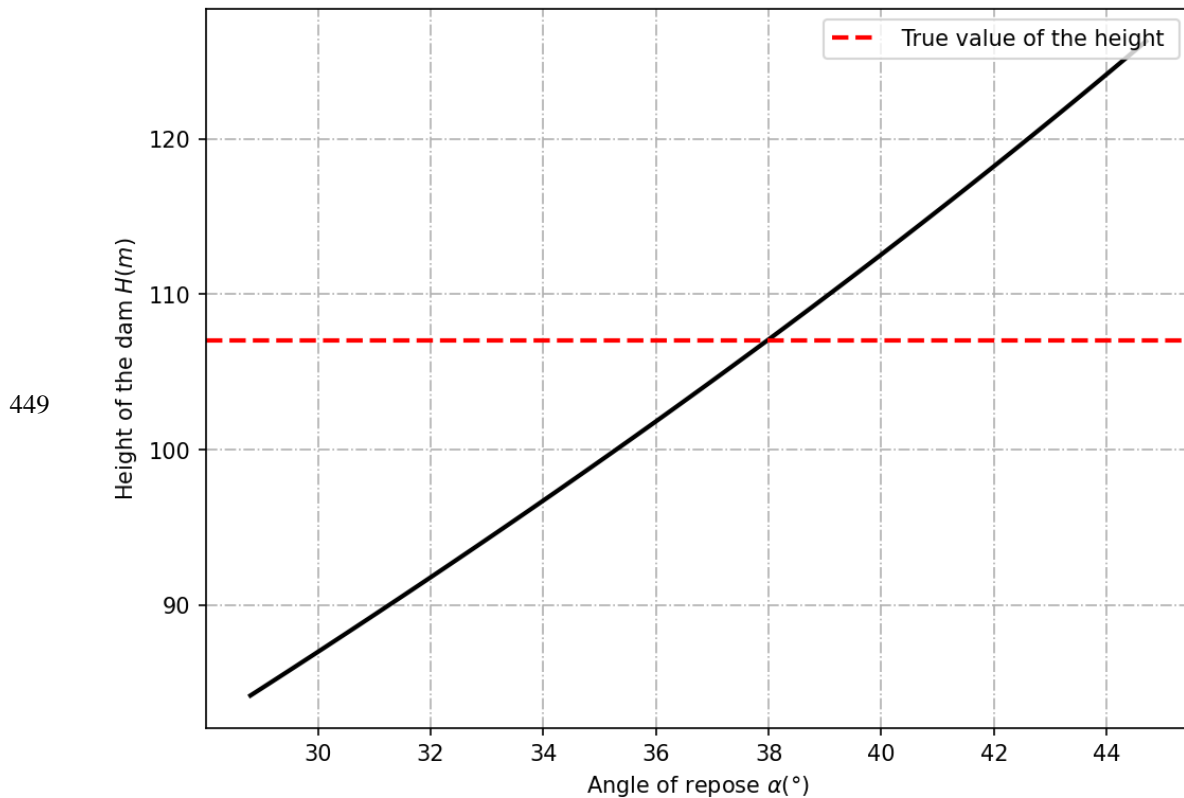
432 elevation of the dam bottom, sensitivity analysis of these two parameters will be conducted on H_m
 433 directly.
 434 In order to analyze the sensitivity to these parameters , we take Baige landslide dam as an example. And
 435 the variation of the prediction result with the change of parameters is shown as follow:
 436



437
 438 Fig 14 the relationship between the predicted result and the input parameters.
 439

440 As can be seen from Fig 14, with other parameters unchanged, the greater the observable length of the
 441 dam and the difference of height between the lake level and dam bottom, the higher the dam crest. The
 442 crest of the dam gets lower as the slope angle of landslide surface and the inclination angle of the riverbed
 443 rise. The slope foot of the dam is mainly affected by the angle of landslide surface and inclination angle
 444 of the riverbed. The smaller the slope foot, the smaller the height of the dam. The calculated results are
 445 in good agreement with expectations.

446 Meantime, it can be found that these parameters all have an impact of about 10% on the final prediction
 447 results. So, it is necessary to be careful to determine these parameters. Possible methods to reduce errors
 448 include repeat procedures and more reliable historical data.



450 Fig 15 the relationship between the predicted result and the angle of repose.

451

452 Finally, it is found that the angle of repose of the dam body has a significant influence on the height of
 453 the dam (Fig 15). The greater the angle of repose, the greater the estimate of dam height. According to
 454 Wang's field survey, the angle of repose of the landslide dams in Wenchuan earthquake ranges from 28.8°
 455 to 44.7°, with an average value of 35.5°(Wang et al., 2013). In the absence of the historical date, the
 456 average value proposed by Wang can be used. However, in this way, the difference between the final
 457 result and the true value can be about 30% in the worst case. Therefore, on the premise of sufficient
 458 disaster relief resources, it is better to make a bad estimate of the repose angle, so as not to make a wrong
 459 judgment on the hazard. On the other hand, it is also possible to check the repose angle of the material
 460 in advance in landslide prone area, so as to make a quick hazard assessment after the landslide.

461 5.3. Influence of image solution

462 The remote sensing image used in the case of Baige landslide dam is Beijing-1 with a resolution of 0.8m
 463 and the pre-landslide DEM is SRTM V3 with a resolution of 30m. As more and more remote sensing
 464 data are available, in addition to satellite-based remote sensing platform, small UAV remote sensing
 465 platform can also be well applied to this procedure. As different sensors and remote sensing platforms
 466 may have different resolutions, we use interpolation to obtain images with different resolutions to explore
 467 the appropriate resolution for this procedure (Table 4, Table 5).

468

Resolution	Input						
	H_1 (m)	H_0 (m)	H_m (m)	L_m (m)	α (°)	θ (°)	φ (°)
0.8	2944	2860	84	567	30.65	0.11	35.5
5	2946	2861	70	545	28.58	0.10	35.5
15	2943	2856	73	562	29.44	0.09	35.5
30	2956	2862	84	540	29.10	0.16	35.5

469 Table 4 the parameters obtained through different resolution image, where H_1 is the elevation of the
470 lake level, H_0 is the elevation of the dam bottom, H_m is H_1 minus H_0 , L_m is the length of the
471 dam that can be observed in the image, α is the slope angle of landslide surface, θ is the
472 inclination angle of the riverbed and φ is the angle of repose

Resolution	Output		Accuracy
	H (m)	True value H (m)	Error(m)
0.8	2964.2	2967	2.8
5	2964.7	2967	2.3
15	2961.6	2967	5.4
30	2960.5	2967	6.5

473 Table 5 the predicted result of image with different resolutions

474

475 As we discussed before, the main parameters in this procedure include the length of the dam that can be
476 observed, the lake level, the elevation of the dam bottom, the slope angle of landslide surface and the
477 inclination angle of the riverbed. Obviously, the resolution of the image will affect all of these five (Table
478 4), but mainly affect the determining of length of the dam that can be observed and the lake level. In
479 general, the higher the resolution, the more accurate the prediction results obtained. When the resolution
480 drops from 0.8m to 30m, the error of prediction results changes from 2.8m to 6.5m, as shown in Table 5.
481 But for the procedure this paper proposed, image with resolution of 5m is sufficient for a good estimate
482 of the dam height.

483 There is no doubt that the resolution and quality of DEM data are very important for this procedure.
484 However, due to the lack of comparative data, this paper does not conduct in-depth discussion on it. For
485 this part, Dong has had relevant discussions in his research(Dong et al., 2014) for readers' reference.

486 5.4. Other discussion

487 In this study, the predicting model is mainly based on the formation mechanism of the barrier dam
488 combined with a single remote sensing image and pre-landslide DEM to quickly predict the essential
489 parameters of the landslide dam hazard. Therefore, a more comprehensive assessment of the reliability of
490 formation mechanism has also been carried out. It is found that most laws can be applied well, but
491 formula (3) has greater limitations in fitting the "cut-top" effect. In Wu's experiment, the "cut-top" effect
492 fitting is mainly determined by the slope angle of landslide surface. Actually, the angle between the

493 riverbed plane and slop surface of the dam should be determined by its landslide potential energy,
494 landslide length, and landslide angle(Grasselli et al., 2000; Xu et al., 2013; Iverson et al., 2015). In
495 addition to the slope angle of landslide surface, the length of the landslide and potential energy are equally
496 important. In Wu's formula, only the slope angle of landslide surface is considered, so more experiments
497 are needed to improve the fitting.

498 As there are not enough theoretical researches to support the prediction of the lowest elevation of the
499 dam crest, the method proposed in this paper still has certain limitations. In addition, the mechanism of
500 the relationship between the highest elevation of the dam crest and the lowest elevation of the dam crest
501 is not clear. In most cases, when it comes to the height of a barrier lake, usually only the highest or lowest
502 elevation is recorded, resulting in fewer complete records of both parameters. As the recording in most
503 cases is not completed, only a small number of cases are used to carry out the fitting. Therefore, this
504 aspect still needs more work and related researches to support relevant predictions.

505

506 **6. Conclusion**

507 This research proposes a procedure based on a single remote sensing image to predict the height of the
508 dam crest and rapidly assess the hazard. With the after-landslide remote sensing image, it only takes no
509 more than one human hour to complete the whole procedure. Compared with Dong's procedure(, this
510 method only requires only one single remote sensing image and has a wider applicability. In view of the
511 large topographic changes in the landslide area, a more reasonable method of using the pre-landslide
512 DEM is proposed. Even the use of poor-quality DEM can complete the relevant prediction and hazard
513 assessment. In the case of Baige Landslide Dam, by extracting the barrier lake surface elevation and
514 determining the bottom elevation of the dam, the prediction of the highest elevation of the dam crest is
515 completed, and the difference between the predicted results and the measured data is within 3m. Since
516 the lowest point of the dam crest determines the potential maximum volume of the barrier lake, we based
517 on historical records find that the height of the highest point and the lowest point of the landslide dam
518 crest basically conforms to the linear relationship. The relationship is expressed as a formula (9) through
519 unary fitting. The prediction result of the lowest elevation of the crest of the Baige Landslide Dam is
520 2964.2m, whose error is 2.8m compared to data from field survey, 2967 m. And in the case of Hongshiyan
521 landslide dam, the error of predicting result of dam top elevation is 5.3m.

522 In the discussion part, some essential parameters of landslide dam, such as the volume of the dam, the
523 stability of the dam and the potential maximum flood peak of the dam break without treatment, is
524 calculated based on the predicting result, which is basically consistent with the true value. The sensitivity
525 of the parameters used in this method is analyzed, and it is found that the repose angle of the landslide
526 material can affect the prediction result up to 30%. Therefore, the repose angle should be carefully
527 determined when using this procedure for related applications. Finally, through experiment with different
528 resolutions of remote sensing images, we find that as the resolution becomes lower, the accuracy of this

529 method decreases. The resolution of 5m and above is a reasonable range for applying this method,
530 otherwise it will be difficult to distinguish the dam body and the water boundary.

531 **Data availability**

532 The data are available from the authors upon request.

533 **Author Contributions**

534 WJZ designed the experiments, and YZ carried them out. SXW and FTW gave some very important
535 suggestions on basic knowledge of landslide dams. LTW, WLL, ZQ and JFZ helped to operate the whole
536 procedure. QG, ZQW helped with some figures, and YBX provided some remote sensing images. FTW
537 prepared the manuscript with contributions from all co-authors.

538 **Competing interests**

539 The authors declare that they have no conflict of interest.

540 **Acknowledgements**

541 We appreciate the constructive reviews provided by three anonymous reviewers and editor Hans-Balder
542 Havenith. The authors acknowledge the support from the National Key R&D Program of China under
543 Grant 2017YFB0504101 and Grant 2021YFB3901201.

544 **Financial support**

545 This research has been supported by the National Key R&D Program of China under Grant
546 2017YFB0504101 and Grant 2021YFB3901201.

547
548
549

550 Reference

- 551 Adams, J.: Earthquake-dammed lakes in New Zealand, 9, 215–219, 1981.
- 552 Anon: Exploring machine learning potential for climate change risk assessment, 103752,
553 <https://doi.org/10.1016/j.earscirev.2021.103752>, 2021.
- 554 Ayalew, L. and Yamagishi, H.: The application of GIS-based logistic regression for landslide
555 susceptibility mapping in the Kakuda-Yahiko Mountains, Central Japan, *Geomorphology*, 65, 15–31,
556 <https://doi.org/10.1016/j.geomorph.2004.06.010>, 2005.
- 557 Braun, A., Cuomo, S., Petrosino, S., Wang, X., and Zhang, L.: Numerical SPH analysis of debris flow
558 run-out and related river damming scenarios for a local case study in SW China, *Landslides*, 15, 535–
559 550, <https://doi.org/10.1007/s10346-017-0885-9>, 2018.
- 560 Briaud, J.-L.: Case Histories in Soil and Rock Erosion: Woodrow Wilson Bridge, Brazos River Meander,
561 Normandy Cliffs, and New Orleans Levees, 134, 1425–1447, [https://doi.org/10.1061/\(ASCE\)1090-0241\(2008\)134:10\(1425\)](https://doi.org/10.1061/(ASCE)1090-0241(2008)134:10(1425)), 2008.
- 563 Canuti, P., Casagli, N., Ermini, L., Fanti, R., and Farina, P.: Landslide activity as a geoinicator in Italy:
564 significance and new perspectives from remote sensing, *Environ. Geol.*, 45, 907–919,
565 <https://doi.org/10.1007/s00254-003-0952-5>, 2004.
- 566 Cao, Z., Yue, Z., and Pender, G.: Landslide dam failure and flood hydraulics. Part II: coupled
567 mathematical modelling, 59, p.1021-1045, 2011.
- 568 Chen, C.-Y., Chen, T.-C., Yu, F.-C., and Hung, F.-Y.: A landslide dam breach induced debris flow – a case
569 study on downstream hazard areas delineation, *Env Geol*, 47, 91–101, <https://doi.org/10.1007/s00254-004-1137-6>, 2004.
- 571 Chen, X. and Lu: Geomatics-based Method Research on Capacity Calculation of Quake Lake, 2008.
- 572 Chen, Z., Chen, S., and Wang, L.: Back analysis of the breach flood of the 11.03 Baige barrier lake at the
573 Upper Jinsha River, 2020.
- 574 Chen, Z., Zhou, H., Ye, F., Liu, B., and Fu, W.: The characteristics, induced factors, and formation
575 mechanism of the 2018 Baige landslide in Jinsha River, Southwest China, *Catena*, 203, 105337,
576 <https://doi.org/10.1016/j.catena.2021.105337>, 2021.
- 577 Costa, J. E. and Schuster, R. L.: The formation and failure of natural dams, 100, 1054–1068,
578 [https://doi.org/10.1130/0016-7606\(1988\)100<1054:TFAFON>2.3.CO;2](https://doi.org/10.1130/0016-7606(1988)100<1054:TFAFON>2.3.CO;2), 1988.
- 579 Costa, J. E. and Schuster, R. L.: Documented historical landslide dams from around the world,
580 Documented historical landslide dams from around the world, U.S. Geological Survey, Vancouver, WA,
581 <https://doi.org/10.3133/ofr91239>, 1991.
- 582 Cui, P., Zhu, Y., Han, Y., Chen, X., and Zhuang, J.: The 12 May Wenchuan earthquake-induced landslide
583 lakes: distribution and preliminary risk evaluation, *Landslides*, 6, 209–223,
584 <https://doi.org/10.1007/s10346-009-0160-9>, 2009.

- 585 Dong, J.-J., Tung, Y.-H., Chen, C.-C., Liao, J.-J., and Pan, Y.-W.: Logistic regression model for predicting
586 the failure probability of a landslide dam, *Engineering Geology*, 117, 52–61,
587 <https://doi.org/10.1016/j.enggeo.2010.10.004>, 2011a.
- 588 Dong, J.-J., Tung, Y.-H., Chen, C.-C., Liao, J.-J., and Pan, Y.-W.: Logistic regression model for predicting
589 the failure probability of a landslide dam, *Engineering Geology*, 117, 52–61,
590 <https://doi.org/10.1016/j.enggeo.2010.10.004>, 2011b.
- 591 Dong, J.-J., Lai, P.-J., Chang, C.-P., Yang, S.-H., Yeh, K.-C., Liao, J.-J., and Pan, Y.-W.: Deriving
592 landslide dam geometry from remote sensing images for the rapid assessment of critical parameters
593 related to dam-breach hazards, *Landslides*, 11, 93–105, <https://doi.org/10.1007/s10346-012-0375-z>,
594 2014.
- 595 Ermini, L. and Casagli, N.: Prediction of the behaviour of landslide dams using a geomorphological
596 dimensionless index, 28, 31–47, <https://doi.org/10.1002/esp.424>, 2003.
- 597 Fan, X., van Westen, C. J., Xu, Q., Gorum, T., and Dai, F.: Analysis of landslide dams induced by the
598 2008 Wenchuan earthquake, *Journal of Asian Earth Sciences*, 57, 25–37,
599 <https://doi.org/10.1016/j.jseaes.2012.06.002>, 2012.
- 600 Fan, X., Dufresne, A., Siva Subramanian, S., Strom, A., Hermanns, R., Tacconi Stefanelli, C., Hewitt, K.,
601 Yunus, A. P., Dunning, S., Capra, L., Geertsema, M., Miller, B., Casagli, N., Jansen, J. D., and Xu, Q.:
602 The formation and impact of landslide dams – State of the art, *Earth-Science Reviews*, 203, 103116,
603 <https://doi.org/10.1016/j.earscirev.2020.103116>, 2020.
- 604 Fan, X., Dufresne, A., and Whiteley, J.: Recent technological and methodological advances for the
605 investigation of landslide dams, 218, 103646, <https://doi.org/10.1016/j.earscirev.2021.103646>, 2021.
- 606 Grasselli, Y., Herrmann, H. J., Oron, G., and Zapperi, S.: Effect of impact energy on the shape of granular
607 heaps, *GM*, 2, 97–100, <https://doi.org/10.1007/s100350050039>, 2000.
- 608 Han, Y., Chun, Q., and Wang, H.: Quantitative safety evaluation of ancient Chinese timber arch lounge
609 bridges, *Journal of Wood Science*, 68, 4, <https://doi.org/10.1186/s10086-022-02011-y>, 2022.
- 610 Iverson, R. M., George, D. L., Allstadt, K., Reid, M. E., Collins, B. D., Vallance, J. W., Schilling, S. P.,
611 Godt, J. W., Cannon, C. M., and Magirl, C. S.: Landslide mobility and hazards: implications of the 2014
612 Oso disaster, 2015.
- 613 Li, H., Qi, S., Chen, H., Liao, H., Cui, Y., and Zhou, J.: Mass movement and formation process analysis
614 of the two sequential landslide dam events in Jinsha River, Southwest China, *Landslides*, 16, 2247–2258,
615 <https://doi.org/10.1007/s10346-019-01254-z>, 2019.
- 616 Li, T. C., Schuster, R. L., and Wu, J. S.: Landslide dams in south-central China, 1986.
- 617 Luo, J., Pei, X., Evans, S. G., and Huang, R.: Mechanics of the earthquake-induced Hongshiyuan landslide
618 in the 2014 Mw 6.2 Ludian earthquake, Yunnan, China, *Engineering Geology*, 251, 197–213,
619 <https://doi.org/10.1016/j.enggeo.2018.11.011>, 2019.
- 620 Meng, C.-K., Chen, K.-T., Niu, Z.-P., Di, B.-F., and Ye, Y.-J.: Influence of Internal Structure on Breaking
621 Process of Short-Lived Landslide Dams, 9, 2021.
- 622 Mora Castro, S.: The 1992 Río Toro landslide dam, Costa Rica, *Landslide News*, 1993.
- 623 Morgenstern, R., Massey, C., Rosser, B., and Archibald, G.: Landslide Dam Hazards: Assessing Their
624 Formation, Failure Modes, Longevity and Downstream Impacts, 2021.
- 625 Peng, M. and Zhang, L. M.: Breaching parameters of landslide dams, *Landslides*, 9, 13–31,
626 <https://doi.org/10.1007/s10346-011-0271-y>, 2012.

- 627 Ruan, H., Chen, H., Wang, T., Chen, J., and Li, H.: Modeling Flood Peak Discharge Caused by
628 Overtopping Failure of a Landslide Dam, 13, 921, <https://doi.org/10.3390/w13070921>, 2021.
- 629 Shen, D., Shi, Z., Peng, M., Zhang, L., and Jiang, M.: Longevity analysis of landslide dams, 17, 2020.
- 630 Shi, Z., Ma, X., and Peng, M.: STATISTICAL ANALYSIS AND EFFICIENT DAM BURST
631 MODELLING OF LANDSLIDE DAMS BASED ON A LARGE-SCALE DATABASE, 33, 1780–1790,
632 2014.
- 633 Walder, J. S. and OConnor, J. E.: Methods for predicting peak discharge of floods caused by failure of
634 natural and constructed earthen dams, *Water Resour. Res.*, 33, 2337–2348,
635 <https://doi.org/10.1029/97WR01616>, 1997.
- 636 Wang, J.-J., Zhao, D., Liang, Y., and Wen, H.-B.: Angle of repose of landslide debris deposits induced
637 by 2008 Sichuan Earthquake, *Eng. Geol.*, 156, 103–110, <https://doi.org/10.1016/j.enggeo.2013.01.021>,
638 2013.
- 639 Wang, Z. H. and Lu, J. T.: Satellite monitoring of the Yigong landslide in Tibet, China, in: *Earth
640 Observing Systems VII*, Bellingham, 34–38, <https://doi.org/10.1117/12.453739>, 2002.
- 641 Wu, H., Nian, T., Chen, G., Zhao, W., and Li, D.: Laboratory-scale investigation of the 3-D geometry of
642 landslide dams in a U-shaped valley, *Engineering Geology*, 265, 105428,
643 <https://doi.org/10.1016/j.enggeo.2019.105428>, 2020.
- 644 Xu, W.-J., Xu, Q., and Wang, Y.-J.: The mechanism of high-speed motion and damming of the
645 Tangjiashan landslide, *Eng. Geol.*, 157, 8–20, <https://doi.org/10.1016/j.enggeo.2013.01.020>, 2013.
- 646 Yang, S.-H., Pan, Y.-W., Dong, J.-J., Yeh, K.-C., and Liao, J.-J.: A systematic approach for the assessment
647 of flooding hazard and risk associated with a landslide dam, *Nat Hazards*, 65, 41–62,
648 <https://doi.org/10.1007/s11069-012-0344-9>, 2013.
- 649 Yunjian, G., Siyuan, Z., Jianhui, D., Zhiqiu, Y., and Mahfuzur, R.: Flood assessment and early warning
650 of the reoccurrence of river blockage at the Baige landslide, *J. Geogr. Sci.*, 31, 1694–1712,
651 <https://doi.org/10.1007/s11442-021-1918-9>, 2021.
- 652 Zhang, L., Xiao, T., He, J., and Chen, C.: Erosion-based analysis of breaching of Baige landslide dams
653 on the Jinsha River, China, in 2018, 2019.
- 654 Zhong, Q. M., Chen, S. S., Mei, S. A., and Cao, W.: Numerical simulation of landslide dam breaching
655 due to overtopping, *Landslides*, 15, 1183–1192, <https://doi.org/10.1007/s10346-017-0935-3>, 2018.
- 656 Zhou, J., Cui, P., and Hao, M.: Comprehensive analyses of the initiation and entrainment processes of
657 the 2000 Yigong catastrophic landslide in Tibet, China, *Landslides*, 13, 39–54,
658 <https://doi.org/10.1007/s10346-014-0553-2>, 2016.
- 659 Zhou, X., Chen, Z., Yu, S., Wang, L., Deng, G., Sha, P., and Li, S.: Risk analysis and emergency actions
660 for Hongshiyuan barrier lake, *Nat Hazards*, 79, 1933–1959, <https://doi.org/10.1007/s11069-015-1940-2>,
661 2015.
- 662